

Eu(III), Sm(III), Np(V), Pu(V), and Pu(IV) sorption to calcite

By M. Zavarin*, S. K. Roberts, N. Hakem, A. M. Sawvel and A. B. Kersting

Lawrence Livermore National Laboratory, 7000 East Avenue, L-221, Livermore, California, 94551 USA

(Received April 18, 2004; accepted in revised form July 14, 2004)

Sorption / Neptunium / Plutonium / Samarium / Europium / Calcite

Summary. The sorption behavior of Eu(III), Sm(III), Np(V), Pu(V), and Pu(IV) in the presence of calcite and as a function of pH and carbonate alkalinity was measured by batch sorption experiments. Eu(III) and Sm(III) sorption is similar, consistent with their observed aqueous speciation and precipitation behavior. For both rare earth elements, sorption decreases at the highest and lowest measured pHs. This is likely the result of speciation changes both of the calcite surface and the sorber. An increase in the equilibrium CO₂(g) fugacity results in a shift in the sorption behavior to lower pH, consistent with a predicted aqueous speciation shift. Np(V) and Pu(V) sorption exhibited a strong pH dependence. For Np(V), K_d s range from 0 to 217 mL/g suggesting that carbonate aqueous speciation as well as changes in the calcite surface speciation greatly affect Np(V) sorption to the calcite surface. Similar behavior was found for Pu(V). Pu(IV) sorption is also strongly pH dependent. Sorption decreases significantly at high pH as a result of Pu-carbonate complexation in solution. A surface complexation model of Sm(III), Eu(III), Np(V), Pu(V), and Pu(IV) sorption to the calcite surface was developed based on the calcite surface speciation model of Pokrovsky and Schott [1]. Sorption data were fit using one or two surface species for each sorber and could account for the effect of pH and CO₂(g) fugacity on sorption. A relatively poor model fit to Pu(IV) sorption data at high pH may result from our poor understanding of Pu(IV)-carbonate aqueous speciation. While our surface complexation model may not represent a unique solution to the sorption data, it illustrates that a surface complexation modeling approach may adequately describe the sorption behavior of a number of radionuclides at the calcite surface over a range of solution conditions.

1. Introduction

The interaction of radionuclides with calcite is likely to affect radionuclide transport behavior in the geosphere at a number of radionuclide contaminated sites. For example, calcite minerals are abundant in the caliche layer below the Hanford Reservation, USA [2] and may provide a transport barrier for certain radionuclides. Calcite is found in great abundance at the Marshall Islands, a location used for atmospheric testing of nuclear devices in the 1940's and

1950's [3]. Calcite is also found in relatively large quantities in the subsurface of the Nevada Test Site and along the fracture surfaces in the host rock at the proposed Yucca Mountain nuclear waste repository, USA [4].

The pH and carbonate alkalinity were previously shown to affect divalent cation sorption to calcite [5] and are likely to affect REE and actinide sorption as well. For divalent cations, sorption tends to decrease with pH most likely as a result of the increasing positive charge on the calcite surface. Carbonate alkalinity is likely to affect sorption to calcite as a result of both aqueous complexation with REEs and actinides and competitive carbonate sorption to the calcite surface.

In this paper, Sm, Eu, Np, and Pu sorption as a function of pH and carbonate alkalinity are reported and compared to available published data. A Sm, Eu, Np, and Pu surface complexation (SC) model based on recent models of calcite surface speciation [1, 6, 7] is developed. While the SC reaction constants do not constitute a unique solution (significantly more sorption data along with spectroscopic information would be required to develop a well calibrated SC model), they provide guidance in understanding the behavior of the radionuclides as a function of pH and carbonate alkalinity. The SC model of the calcite surface can be used to explain the effects of pH and carbonate alkalinity on Sm, Eu, Np, and Pu sorption over the range of conditions examined here. The modeling reported here is believed to be one of the first attempts to describe radionuclide sorption to calcite using a surface complexation model.

1.1 Background – REE and actinide sorption to calcite

Limited data available in the literature regarding REE and actinide sorption to calcite suggest that calcite can be an important sorbent. For example, the sorption of Np(V) to a variety of minerals was reported at pH 8 and in distilled water and seawater [8]. It was found that Np(V) sorbs to calcite more strongly than to most minerals, with the order of decreasing sorption strength being: aragonite \geq calcite $>$ goethite $>$ MnO₂ \approx clays. The data suggest that calcite is an important sorbent for Np(V) under these conditions. The sorption of Pu(V) to a variety of minerals was reported under similar solution conditions [9]. Pu(V) was found to sorb to calcite only slightly less than to goethite. Unlike Np(V) and Pu(V), sorption of U(VI) to calcite (as a function of both pH and carbonate alkalinity) appears to be quite weak [10].

* Author for correspondence (E-mail: zavarin1@llnl.gov).

Trivalent actinides and REEs sorb very strongly to calcite. For example, in seawater, Am(III) sorbs to calcite with a K_d greater than 10^5 mL/g [11]. A Nd(III) K_d of $10^{3.4}$ mL/g was reported in pure water at 50 °C [29]. The sorption and coprecipitation of trivalent REEs to calcite [12] is quite strong under seawater conditions with the K_d decreasing slightly with REE atomic number.

Calcite coprecipitation and sorption data were recently critically evaluated using an empirical partitioning coefficient model [13]. Radionuclide partitioning coefficients were correlated to known chemical properties of the radionuclides (radionuclide solubility products and ionic radii) to provide a set of empirical partitioning coefficients. However, these partitioning coefficients do not account for the effects of pH and carbonate alkalinity (or any other surface or solution speciation effects) and can, therefore, be regarded as limited in their applicability.

Some spectroscopic information regarding the sorption behavior of trivalent actinide and REEs is available in the literature. Time-resolved laser fluorescence spectroscopy measurements of Cm(III) sorption to calcite suggest that Cm(III) is initially sorbed at the hydrated calcite surface with coordination similar to the aqueous tetracarbonato species [30]. Over time, Cm(III) was shown to slowly dehydrate and incorporate into the calcite structure, on the scale of months [30]. Similarly, Eu(III) was found to be predominantly sorbed as a hydrated surface species on calcite with only a small fraction apparently incorporated into the calcite solid [31]. The nature of the hydrated calcite surface was suggested to be composed of several near-surface layers of calcite, as initially suggested in [32] for Cd²⁺ sorption. However, recent spectroscopic examination of the calcite surface suggests that hydration only occurs at the termination of the bulk structure (see [33] and references therein). Recent Cd²⁺ uptake experiments suggest that, adsorption at the surface occurs initially and is later followed by solid-state diffusion [34]. This is consistent with Cm(III) sorption data reported in [30] and can explain Eu(III) sorption data reported in [31]. The sorption experiments reported here focus on adsorption at the calcite–water interface. For adsorption modeling purposes, sorption reaction times were kept short (24 to 48 hours) to ensure that adsorption was distinguished from radionuclide incorporation (by precipitation, solid-state diffusion or other processes) into the solid. In some cases, sorption experiment times were extended to up to 30 days to examine whether radionuclide incorporation over longer times would be observed.

1.2 Background – calcite surface complexation modeling

There are many models that have been used to describe SC reactions (non-electrostatic, constant capacitance, diffuse layer, triple layer, and others). However, a description of the calcite mineral surface based on a SC model was proposed only recently [7]. Previously, most sorption reactions on the calcite surface were described either as surface exchange reactions (partitioning coefficients) or simply reported as K_d distribution coefficients. For example, Zachara *et al.* [5] described the sorption of a variety of divalent cations on the calcite surface as an exchange reaction between surface Ca

ions and the divalent cations (*i.e.* $>Ca^{2+} + M^{2+} \rightleftharpoons >M^{2+} + Ca^{2+}$). While this partitioning model works well for the exchange of divalent cations with surface Ca ions as well as the exchange of selenite with surface carbonate [14], the use of a simple partitioning model in cases where the sorbing ion has a charge that is different from Ca²⁺ (or CO₃²⁻) results in a reaction charge imbalance. Van Cappellen *et al.* [7] proposed a SC model for calcite that would account for changes in the surface charge and surface speciation as a function of solution conditions. This SC model was further evaluated and refined for the calcite and dolomite surfaces using diffuse reflectance infrared (DRIFT) spectroscopy [6]. More recently, a SC model for a number of divalent metal carbonates was developed based on additional electrophoretic mobility and extrapolated aqueous speciation data [1]. Marin-Garin *et al.* [34] effectively used both a surface exchange and a SC model to describe Cd²⁺ sorption to the calcite surface. Using stirred flow-through reactors, they were able to distinguish between short-term surface adsorption and long-term incorporation of Cd(II) into the calcite solid. We used the most recent SC model [1] to simulate Sm, Eu, Np, and Pu sorption to the calcite surface as a function of pH and carbonate alkalinity. The experiment reaction time was kept relatively short to ensure that adsorption to the calcite surface was the predominant sorption mechanism.

2. Methods

2.1 Calcite sorbent

Reagent-grade calcite was aged for several months in 0.02 mol/L NaHCO₃(aq) to establish calcite crystallites with a more uniform particle diameter. This recrystallization procedure was used by Zachara *et al.* [5] to reduce the likelihood of recrystallization effects during sorption experiments. After several months of ageing, the calcite was filtered, washed with distilled water and then dried. The surface area of the calcite, measured by N₂(g) BET, was found to be 0.262 m²/g. SEM analysis of recrystallized calcite showed rhombohedral particles ranging between 4 and 10 micrometers in size, consistent with BET measurements.

2.2 Calcite equilibrated batch sorption solutions

Two sets of solutions were prepared for batch sorption experiments. The first set of solutions was prepared at equilibrium with atmospheric CO₂(g) (0.03%). The second set of solutions was prepared at equilibrium with 1% CO₂(g).

For the 0.03% CO₂(g) solutions, ten solutions ranging from pH 7.50 to 9.75 (at 25 °C) were prepared by mixing HCl, Na₂CO₃, CaCl₂, and NaCl to achieve the desired solution composition and an ionic strength of 0.1. These solutions were then bubbled in air (0.03% CO₂(g)), calcite was added to the solutions to ensure calcite equilibrium, and the solution pH was adjusted with Na₂CO₃ or HCl using a pH-stat apparatus until a stable solution pH was reached (up to several days). A stable pH was assumed to indicate equilibrium. Carbonate alkalinity (measured with an OIC 524 carbon analyzer using direct injection) and calcium concentrations in solution (measured using ICP-AES) were checked to ensure equilibrium with respect to calcite and 0.03% CO₂(g).

For the 1% CO₂(g) solutions, nine solutions ranging from pH 6.75 to 8.75 at 25 °C were prepared by mixing HCl, Na₂CO₃, CaCl₂, and NaCl to achieve the desired solution composition and an ionic strength of 0.1. These solutions were bubbled with 1% CO₂(g) in N₂(g) and adjusted to the prescribed pH using a pH-stat until equilibrium was achieved. All solutions were stored in sealed polyethylene bottles that contained a small amount of calcite to ensure calcite equilibrium in solution. Carbonate alkalinity and calcium concentrations in solution were checked to ensure equilibrium with respect to calcite and 1% CO₂(g).

2.3 Sorption experiments

2.3.1 Sm(III) and Eu(III)

Three sets of batch sorption experiments were performed for Sm(III) and Eu(III). In the first, sorption was measured in the 0.03% CO₂(g) solutions after 24 hour equilibration. In the second, sorption was measured in the 0.03% CO₂(g) solutions after 30 day equilibration. In the third, sorption was measured in the 1% CO₂(g) solutions after 24 hour equilibration. For each set of batch sorption experiments, 40 mL filtered and calcite-equilibrated solution and 50 mg calcite was added to Teflon centrifuge tubes. After 24 hours of equilibration, 40 µL of 10⁻⁴ mol/L Sm(III) or Eu(III) was added to achieve a starting concentration of 10⁻⁷ mol/L. At the end of each set of sorption experiments, solutions were centrifuged instead of filtered to avoid potential losses of Sm(III) or Eu(III) to the filter membranes. Sm and Eu sorption solutions were centrifuged for 11 minutes at 5000 rpm which was expected to remove > 150 nm particles from solution. Based on solubility, formation of real colloids at the experimental Sm/Eu concentrations was not expected. The residual Sm(III) or Eu(III) in solution was measured and used to calculate the percent sorbed. Solution Sm(III), Eu(III), Na, and Ca concentrations were analyzed by ICP-MS or ICP-AES. Solution pH was measured at the start and end of each sorption experiment; no significant change in pH was observed. Blank solutions were run alongside all sorption experiments and showed little or no loss of Eu(III) or Sm(III) to container walls.

2.3.2 Np(V)

The procedure used for Np(V) sorption experiments was the same as for Sm(III) and Eu(III). However, sorption of Np(V) was measured only in 0.03% CO₂(g) solutions and only after 24 hours. The residual Np(V) in solution was measured after centrifugation by scintillation counting. No loss of Np(V) to container walls was observed in blank solutions.

2.3.3 Pu(IV) and Pu(V)

Sorption of Pu(IV) and Pu(V) was measured only in 0.03% CO₂(g) solutions and after 48 hour and 7 day equilibration times. Approximately 125 mg of calcite was added to 25 mL filtered calcite-equilibrated solutions (~ 5 g/L calcite) in polycarbonate centrifuge tubes. Starting Pu concentrations were 5 × 10⁻⁹ mol/L Pu(IV) or 10⁻⁷ mol/L Pu(V). The Pu(IV) solution was composed of a mixture of isotopes dominated by ²³⁹Pu (92.6%) and ²⁴⁰Pu (6.6%). The Pu(V)

solution was composed largely of ²⁴²Pu (99.9%). The residual Pu(IV) or Pu(V) in solution was measured by scintillation counting after centrifugal filtration with ~ 4 nm filters (Aminco, Centricon-SR3). Samples were centrifuge filtered to ensure that real Pu colloids were removed from the supernatant. Parallel blank samples showed little or no loss of Pu to container walls or filters during sorption experiments.

2.4 Aqueous speciation

Aqueous speciation constants used to model the batch sorption solutions were taken from a variety of sources (Table 1). Major ion speciation was calculated using the GEMBOCHS speciation database [15]. Sm(III) and Eu(III) aqueous speciation was taken from Spahiu and Bruno [16] and Hass *et al.* [17]. The Eu(CO₃)₃³⁻ species reported in the GEMBOCHS database was also included in our initial speciation calculations. Under the experimental conditions reported here, the tri-carbonate species was determined not to be significant. The Np(V) and Pu(V) speciation data were taken, in part, from the recent NEA publication of recommended reaction constants [18]. A NpO₂(CO₃)₃⁵⁻ species was not included in the NEA publication but was available in the GEMBOCHS database and compared well with the PuO₂(CO₃)₃⁵⁻ species included in the NEA database. Very little speciation data is available from the recent NEA publication regarding the complexation of Pu(IV) with hydroxide and carbonate ions. Thus, Pu(IV) hydroxide speciation was based on data from Lemire and Tremaine [19]. The Pu(IV) hydroxy-carbonate and carbonate species reaction constants were based on a refitting of the recent data of Rai *et al.* [20] and using the solubility product of amorphous PuO₂(s) reported by Lemire and Tremaine [18]. A summary of these Pu(IV)-carbonate data fits is included in the appendix.

2.5 Surface complexation modeling

Sorption data were fit using a modified version of the fitting program FITEQL [21]. The code was modified to allow for activity correction using the extended Debye-Hückel (b-dot) model, a database link, and code stability for cases of large species matrices such as the ones used here.

The speciation of the calcite surface was based on the constant capacitance model of Pokrovsky and Schott [1]. The capacitance for calcite was based on $I^{1/2}/0.006$ (F/m²) reported in Pokrovsky *et al.* [6] which is high but consistent with the capacitance reported elsewhere [1, 7]. The surface species proposed by Pokrovsky and Schott [1] are listed in Table 2. The reactive site density for >CaOH and >CO₃H sites was based on the geometric site density along the 104 plane of calcite (5 sites/nm²).

3. Results and discussion

3.1 Solution and surface speciation

The batch solution compositions were consistent with model predictions of the total calcium and carbonate in solution at calcite equilibrium (Fig. 1). At 0.03% CO₂(g), total calcium in solution is highest (0.04 mol/L) at pH 7.5 and decreases rapidly with increasing pH. Total carbonate, on the other

Table 1. Predominant aqueous species and their reaction constants.

Reaction	log <i>K</i> (298 K, <i>I</i> = 0)	Reference
$\text{Eu}^{3+} + \text{H}_2\text{O} = \text{EuOH}^{2+} + \text{H}^+$	-7.90	1
$\text{Eu}^{3+} + 2\text{H}_2\text{O} = \text{Eu}(\text{OH})_2^+ + 2\text{H}^+$	-16.37	1
$\text{Eu}^{3+} + 3\text{H}_2\text{O} = \text{Eu}(\text{OH})_3(\text{aq}) + 3\text{H}^+$	-25.41	1
$\text{Eu}^{3+} + 4\text{H}_2\text{O} = \text{Eu}(\text{OH})_4^- + 4\text{H}^+$	-34.51	1
$\text{Eu}^{3+} + \text{HCO}_3^- = \text{EuHCO}_3^{2+}$	2.10	2
$\text{Eu}^{3+} + \text{HCO}_3^- = \text{EuCO}_3^+ + \text{H}^+$	-2.43	2
$\text{Eu}^{3+} + 2\text{HCO}_3^- = \text{Eu}(\text{CO}_3)_2^- + 2\text{H}^+$	-7.76	2
$\text{Eu}^{3+} + 3\text{HCO}_3^- = \text{Eu}(\text{CO}_3)_3^{3-} + 3\text{H}^+$	-18.49	3
$\text{Sm}^{3+} + \text{H}_2\text{O} = \text{SmOH}^{2+} + \text{H}^+$	-7.96	1
$\text{Sm}^{3+} + 2\text{H}_2\text{O} = \text{Sm}(\text{OH})_2^+ + 2\text{H}^+$	-16.50	1
$\text{Sm}^{3+} + 3\text{H}_2\text{O} = \text{Sm}(\text{OH})_3(\text{aq}) + 3\text{H}^+$	-25.91	1
$\text{Sm}^{3+} + 4\text{H}_2\text{O} = \text{Sm}(\text{OH})_4^- + 4\text{H}^+$	-35.01	1
$\text{Sm}^{3+} + \text{HCO}_3^- = \text{SmHCO}_3^{2+}$	2.10	2
$\text{Sm}^{3+} + \text{HCO}_3^- = \text{SmCO}_3^+ + \text{H}^+$	-2.53	2
$\text{Sm}^{3+} + 2\text{HCO}_3^- = \text{Sm}(\text{CO}_3)_2^- + 2\text{H}^+$	-7.86	2
$\text{NpO}_2^+ + \text{H}_2\text{O} = \text{NpO}_2\text{OH}(\text{aq}) + \text{H}^+$	-11.30	3
$\text{NpO}_2^+ + \text{HCO}_3^- = \text{NpO}_2\text{CO}_3^- + \text{H}^+$	-5.37	3
$\text{NpO}_2^+ + 2\text{HCO}_3^- = \text{NpO}_2(\text{CO}_3)_2^{3-} + 2\text{H}^+$	-14.12	3
$\text{NpO}_2^+ + 3\text{HCO}_3^- = \text{NpO}_2(\text{CO}_3)_3^{5-} + 3\text{H}^+$	-25.49	4
$\text{PuO}_2^+ + \text{H}_2\text{O} = \text{PuO}_2\text{OH}(\text{aq}) + \text{H}^+$	-9.73	3
$\text{PuO}_2^+ + \text{HCO}_3^- = \text{PuO}_2\text{CO}_3^- + \text{H}^+$	-5.21	3
$\text{PuO}_2^+ + 3\text{HCO}_3^- = \text{PuO}_2(\text{CO}_3)_3^{5-} + 3\text{H}^+$	-26.00	3
$\text{Pu}^{4+} + \text{H}_2\text{O} = \text{PuOH}^{3+} + \text{H}^+$	-0.78	3
$\text{Pu}^{4+} + 2\text{H}_2\text{O} = \text{Pu}(\text{OH})_2^{2+} + 2\text{H}^+$	-1.66	5
$\text{Pu}^{4+} + 3\text{H}_2\text{O} = \text{Pu}(\text{OH})_3^+ + 3\text{H}^+$	-4.62	5
$\text{Pu}^{4+} + 4\text{H}_2\text{O} = \text{Pu}(\text{OH})_4(\text{aq}) + 4\text{H}^+$	-8.85	5
$\text{Pu}^{4+} + 2\text{H}_2\text{O} = \text{PuO}_2(\text{amorphous}) + 4\text{H}^+$	2.02	3
$\text{Pu}^{4+} + 2\text{H}_2\text{O} + 2\text{HCO}_3^- = \text{Pu}(\text{OH})_2(\text{CO}_3)_2^{2-} + 4\text{H}^+$	-2.75	6
$\text{Pu}^{4+} + 4\text{H}_2\text{O} + 2\text{HCO}_3^- = \text{Pu}(\text{OH})_4(\text{CO}_3)_2^{4-} + 6\text{H}^+$	-25.53	6
$\text{Pu}^{4+} + 4\text{HCO}_3^- = \text{Pu}(\text{CO}_3)_4^{4-} + 4\text{H}^+$	-4.62	7
$\text{Pu}^{4+} + 5\text{HCO}_3^- = \text{Pu}(\text{CO}_3)_5^{6-} + 5\text{H}^+$	-16.30	6
$\text{HCO}_3^- + \text{H}^+ = \text{CO}_2(\text{g}) + \text{H}_2\text{O}$	7.81	4
$\text{HCO}_3^- + \text{H}^+ = \text{CO}_2(\text{aq}) + \text{H}_2\text{O}$	6.34	4
$\text{HCO}_3^- = \text{CO}_3^{2-} + \text{H}^+$	-10.33	4

1: Haas *et al.* [17];

2: Spahiu and Bruno [16];

3: Lemire *et al.* [18];

4: Johnson and Lundeen [15];

5: Lemire and Tremaine [19];

6: Refitted Rai *et al.* [20] data;7: Lemire *et al.* [18] data combined with fitted data of Rai *et al.* [20].**Table 2.** Surface complexation model for calcite based on data from Pokrovsky and Schott [1].

Surface reaction	log <i>K</i> (298 K, <i>I</i> = 0)
$>\text{CO}_3\text{H} = >\text{CO}_3^- + \text{H}^+$	-5.1
$>\text{CO}_3\text{H} + \text{Ca}^{2+} = >\text{CO}_3\text{Ca}^+ + \text{H}^+$	-1.7
$>\text{CaOH} = >\text{CaO}^- + \text{H}^+$	-12.0
$>\text{CaOH} + \text{H}^+ = >\text{CaOH}_2^+$	11.85
$>\text{CaOH} + \text{HCO}_3^- + \text{H}^+ = >\text{CaHCO}_3 + \text{H}_2\text{O}$	13.17
$>\text{CaOH} + \text{HCO}_3^{2-} = >\text{CaCO}_3^- + \text{H}_2\text{O}$	6.77

hand, is highest at pH 9.75 (0.075 mol/L) and decreases rapidly with decreasing pH. Speciation at 1% CO₂(g) is similar but shifted to a lower pH. The dominant calcite surface species are controlled by solution conditions. Thus, at high pH, the surface is predicted to be dominated by >CO₃⁻ terminations while at low pH it is dominated by >Ca⁺ or >CaOH₂⁺ terminations. Again, the trends in the surface speciation are similar for the 0.03% and 1% CO₂(g) data but are shifted to lower pH at higher CO₂(g) fugacities. The point of

zero charge (pzc) for calcite at 0.03% CO₂(g) is predicted to be at pH 8.25. At 1% CO₂(g), the pzc is shifted to pH 7.5.

Figs. 2 through 5 present the calculated aqueous speciation of sorbing radionuclides as a function of pH and solution condition. The Sm(III) speciation is essentially identical to that of Eu(III) and is, therefore, not shown. Eu(III) speciation at 0.03% CO₂(g) is dominated by europium mono- and di-carbonate aqueous species; the tri-carbonate concentration is negligible at all but the highest pH (Fig. 2). As in the case of major cation and surface speciation discussed earlier, speciation trends are essentially similar at 1% CO₂(g) but are shifted to a lower pH at the higher CO₂(g) fugacity. However, the contribution of EuOH⁺ and Eu(CO₃)₃³⁻ is diminished.

At 0.03% CO₂(g), Np(V) speciation is dominated by the free NpO₂⁺ ion and the carbonate complexes (Fig. 3). As in the case of Eu(III), the tricarbonate species appears only at the highest pH and at a low relative concentration. The speciation of Pu(V) is expected to be similar to Np(V). However, a formation constant for the PuO₂(CO₃)₂³⁻ species was not found in the literature. Since SC modeling would be ad-

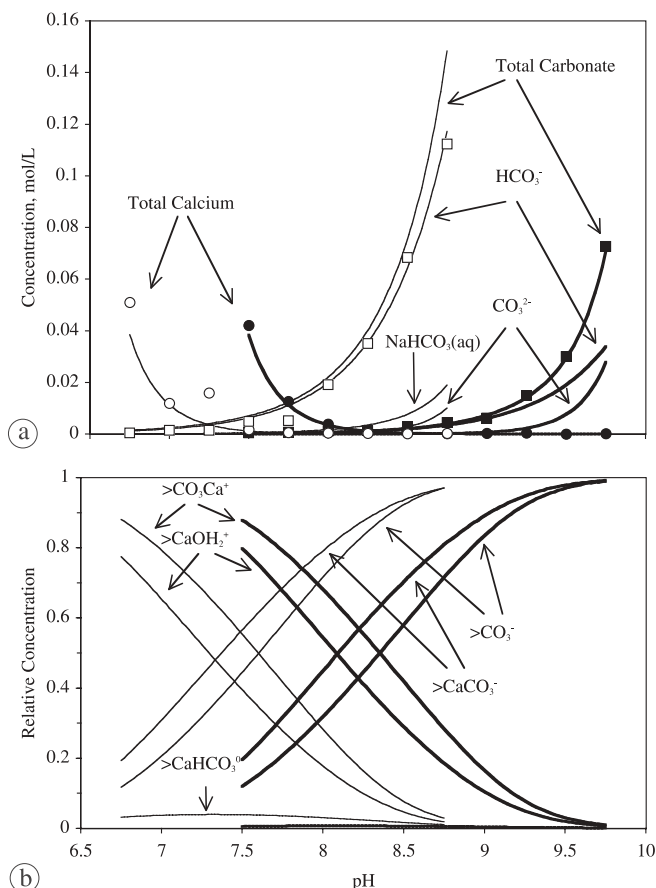


Fig. 1. Predominant (a) aqueous and (b) surface species at calcite saturation conditions. $I = 0.1$ and 0.03% $\text{CO}_2(\text{g})$ (thick lines) or 1% $\text{CO}_2(\text{g})$ (thin lines). \circ and \square represent typical batch solution total calcium and carbonate alkalinity results, respectively (0.03% $\text{CO}_2(\text{g})$ = filled symbols, 1% $\text{CO}_2(\text{g})$ = open symbols).

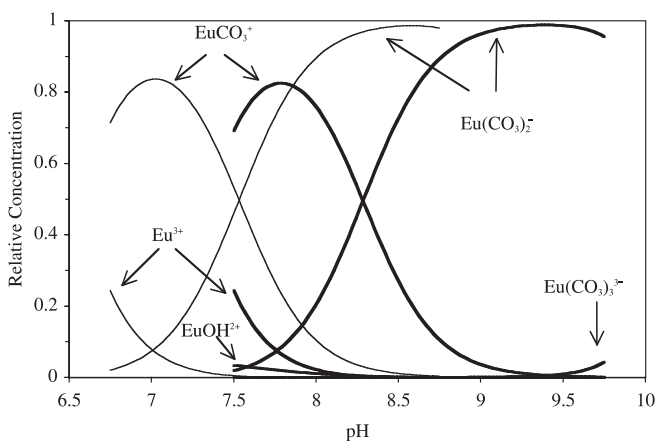


Fig. 2. Speciation of Eu(III) at $I = 0.1$, calcite saturation conditions, and 0.03% $\text{CO}_2(\text{g})$ (thick lines) or 1% $\text{CO}_2(\text{g})$ (thin lines).

versely affected by the missing di-carbonate species, we assumed that the formation constant for the Pu(V) and Np(V) di-carbonate species is essentially the same. With the inclusion of the Pu(V) di-carbonate species, the speciation trends for Np(V) and Pu(V) are quite similar (Figs. 3 and 4). The speciation of Pu(IV) at 0.03% $\text{CO}_2(\text{g})$ is dominated by the di-hydroxy-di-carbonate species (Fig. 5). This is consistent with data of Rai *et al.* [20] and Yamaguchi *et al.* [22], as described in the appendix.

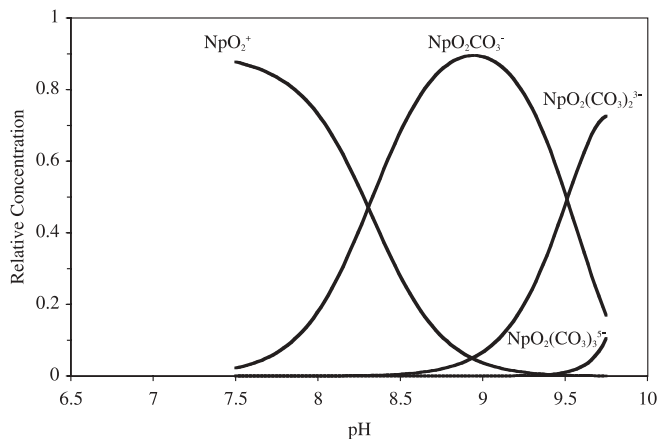


Fig. 3. Speciation of Np(V) at 0.03% $\text{CO}_2(\text{g})$, $I = 0.1$, and calcite saturation conditions.

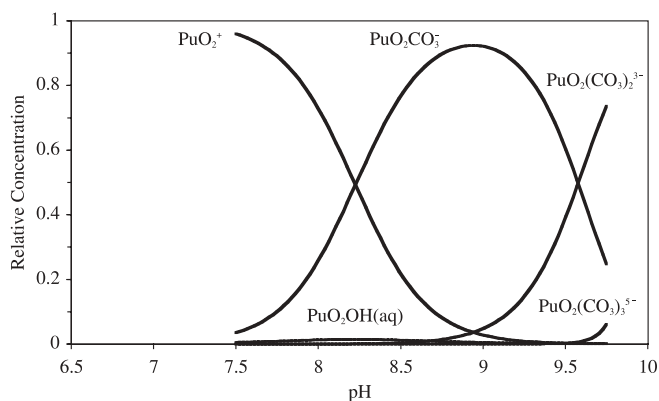


Fig. 4. Speciation of Pu(V) at 0.03% $\text{CO}_2(\text{g})$, $I = 0.1$, and calcite saturation conditions.

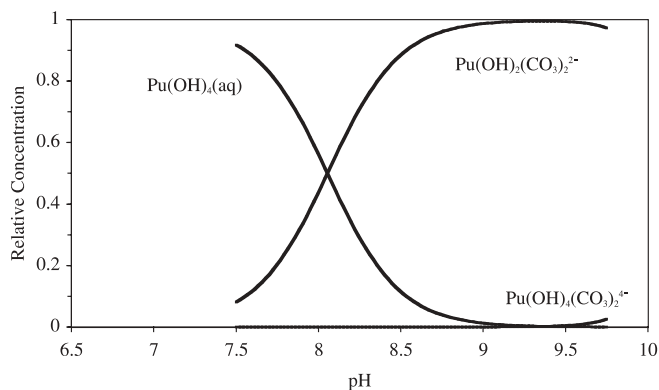


Fig. 5. Speciation of Pu(IV) at 0.03% $\text{CO}_2(\text{g})$, $I = 0.1$, and calcite saturation conditions.

3.2 Eu and Sm sorption

Eu sorption at 0.03% $\text{CO}_2(\text{g})$ varies only slightly as a function of pH (Fig. 6). Sorption does, however, appear to decrease slightly at the lowest and highest pHs (this is more obvious in the 1% $\text{CO}_2(\text{g})$ data). Decreased sorption at lower pH results most likely from an increase in the Eu^{3+} species in solution (Fig. 2) combined with the increasingly positive charge of the calcite surface (Fig. 1). At high pH, the decrease results most likely from the negative charge of the dominant aqueous species ($\text{Eu}(\text{CO}_3)_2^-$ and $\text{Eu}(\text{CO}_3)_3^{3-}$) and an increasingly negative charge of the calcite surface. Never-

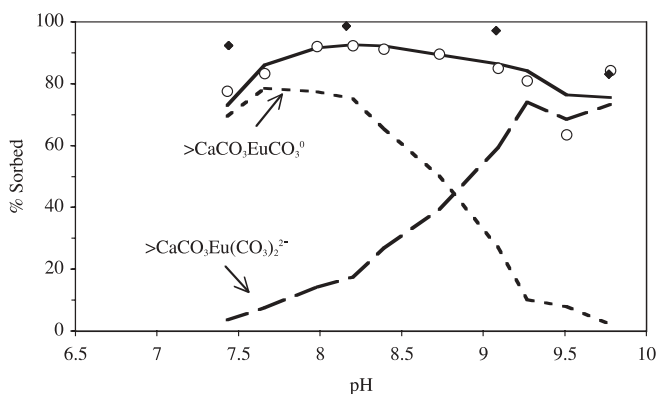


Fig. 6. Eu sorption to calcite at 0.03% CO₂(g) at 24 hours (○) and 30 days (◆). Lines present total and individual species SC model fits to 24 hour data.

theless, the K_d only varies from 1300 to 8800 mL/g for the 24 hour sorption data. At 30 days, sorption has increased to some degree ($K_d = 3600$ to 51 000 mL/g) most likely due to slow incorporation of Eu(III) into the calcite solid (*e.g.* [30]). Eu sorption at 1% CO₂(g) is quite similar to the 0.03% CO₂(g) data but shifted to lower pH (Fig. 7). The shift in the sorption data parallels the predicted shift in surface and aqueous speciation (Fig. 1).

The 24 hour sorption data were modeled using the constant capacitance model described earlier. Fits to the data are shown in Fig. 6 and 7 and reaction constants are listed in Table 3. Two SC reactions are the minimum number that fit the sorption data over the entire pH range and at both CO₂ fugacities (>CaCO₃EuCO₃⁰ and >CaCO₃Eu(CO₃)₂²⁻). Separate fits to the 1% and 0.03% CO₂(g) data resulted in similar reaction constants (Table 3). While our SC model may not represent a unique solution to the sorption data, our modeling suggests that the effect of pH and CO₂ fugacity on sorption can be accounted for using a calcite SC model. Importantly, the SC reactions reported in Table 3 only represent the reaction stoichiometry that best fits the data and

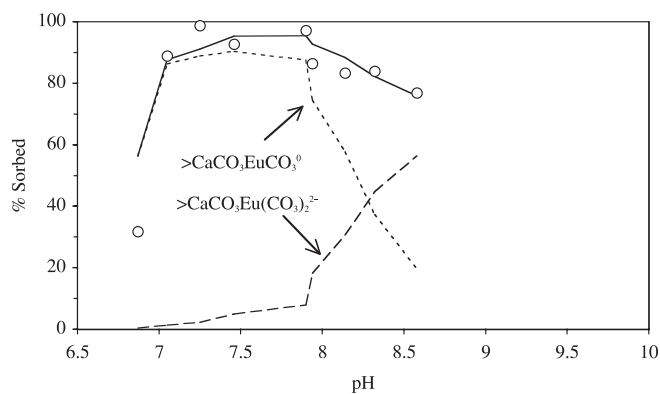


Fig. 7. Eu sorption to calcite at 1% CO₂(g) at 24 hours (○). Lines present total and individual species SC model fits.

do not imply a specific surface coordination. In this report, we attempt to keep modeling in its simplest form using the minimum number of reactions that adequately fit the available sorption data and based exclusively on monodentate (or 1 : 1) SC reactions. The SC model could fit our sorption data equally well using bidentate reactions (as stated in Kosmulski [35], when surface loads are low, fitted monodentate and bidentate surface complexation reactions lead to identical uptake curves and kinetic expressions). Monodentate SC reactions were used so as not to unintentionally imply knowledge of radionuclide surface coordination based on these sorption data. Interestingly, the spectroscopic data reported in [30] for Cm(III) sorption to calcite suggest that adsorbed Cm(III) substitutes for Ca²⁺ at the surface, is coordinated to several CO₃²⁻ ions (with a single CO₃²⁻ in solution), and most resembles a tetracarboxylate coordinated species. Our SC modeling results, while not implying a specific surface coordination, also suggest that sorbed Eu(III) will be primarily coordinated by CO₃²⁻ anions. The value of this modeling is the ability to semi-empirically predict the sorption behavior of Eu over a range of pH and so-

Table 3. Best fit parameters for modeling sorption to calcite.

Reaction ^b	log K (298 K, I = 0)	Data Set
>Ca ⁺ + Eu ³⁺ + 2HCO ₃ ⁻ = >CaCO ₃ EuCO ₃ ⁰ + 2H ⁺	3.49	0.03% CO ₂ (g)
>Ca ⁺ + Eu ³⁺ + 3HCO ₃ ⁻ = >CaCO ₃ Eu(CO ₃) ₂ ²⁻ + 3H ⁺	-2.38	24 h
>Ca ⁺ + Eu ³⁺ + 2HCO ₃ ⁻ = >CaCO ₃ EuCO ₃ ⁰ + 2H ⁺	3.80	1% CO ₂ (g)
>Ca ⁺ + Eu ³⁺ + 3HCO ₃ ⁻ = >CaCO ₃ Eu(CO ₃) ₂ ²⁻ + 3H ⁺	-2.60	24 h
>Ca ⁺ + Sm ³⁺ + 2HCO ₃ ⁻ = >CaCO ₃ SmCO ₃ ⁰ + 2H ⁺	3.90	0.03% CO ₂ (g)
>Ca ⁺ + Sm ³⁺ + 3HCO ₃ ⁻ = >CaCO ₃ Sm(CO ₃) ₂ ²⁻ + 3H ⁺	-1.86	24 h
>Ca ⁺ + Sm ³⁺ + 2HCO ₃ ⁻ = >CaCO ₃ SmCO ₃ ⁰ + 2H ⁺	3.69	1% CO ₂ (g)
>Ca ⁺ + Sm ³⁺ + 3HCO ₃ ⁻ = >CaCO ₃ Sm(CO ₃) ₂ ²⁻ + 3H ⁺	-2.74	24 h
>Ca ⁺ + NpO ₂ ⁺ + 1HCO ₃ ⁻ = >CaCO ₃ NpO ₂ ⁰ + H ⁺	4.36	0.03% CO ₂ (g)
>Ca ⁺ + NpO ₂ ⁺ + 2HCO ₃ ⁻ = >CaCO ₃ NpO ₂ CO ₃ ²⁻ + 2H ⁺	-1.54 ^a	24 h
>Ca ⁺ + PuO ₂ ⁺ + 2HCO ₃ ⁻ = >CaCO ₃ PuO ₂ CO ₃ ²⁻ + 2H ⁺	-1.40	0.03% CO ₂ (g) 48 h
>Ca ⁺ + Pu ⁴⁺ + 2HCO ₃ ⁻ + 2H ₂ O = >CaCO ₃ Pu(OH) ₂ CO ₃ ⁻ + 4H ⁺	15.76	0.03% CO ₂ (g)
>Ca ⁺ + Pu ⁴⁺ + 2HCO ₃ ⁻ + 4H ₂ O = >CaCO ₃ Pu(OH) ₄ CO ₃ ⁻ + 6H ⁺	-8.80	48 h

a: If only the >CaCO₃NpO₂CO₃²⁻ species is included in the fit, log K = -1.14 and the overall fit to the data is still reasonably good;

b: These reactions only imply a reactions stoichiometry and do not imply a reaction mechanism. All reactions were written in terms of the primary species of our database (>Ca⁺, Eu³⁺, HCO₃⁻, Sm³⁺, NpO₂⁺, PuO₂⁺, and Pu⁴⁺, H₂O, and H⁺).

lution conditions and qualitatively understand the factors affecting Eu sorption (and migration in the environment). The reaction stoichiometries cannot be directly compared to spectroscopically-identified surface structures of trivalent cations on calcite. However, the spectroscopic evidence for Cm(III) and Eu(III) coordinated to CO_3^{2-} anions at a hydrated calcite surface [30, 31] is qualitatively similar to the CO_3^{2-} coordinated SC reactions reported in Table 3.

The constant capacitance SC model was based on Pokrovsky and Schott [1]. Over the range of conditions examined here, the relative abundance of the $>\text{CO}_3^-$ and $>\text{CaCO}_3^-$ and the $>\text{CaOH}_2^+$ and $>\text{CO}_3\text{Ca}^+$ surface species as a function of pH are similar (Fig. 1). This is not altogether unreasonable since, upon sorption of Ca^{2+} to a $>\text{CO}_3^-$ site, the resulting surface site can be described as either $>\text{Ca}^+$ or $>\text{CO}_3\text{Ca}^+$ depending on where one defines the surface boundary. This interpretation of the surface was proposed to explain the unusually high capacitance of the calcite surface [23]. In fact, a surface species such as $>\text{CaCO}_3\text{EuCO}_3^0$ should not be distinguished from $>\text{CO}_3\text{EuCO}_3^0$ in our SC model. Furthermore, mechanistically, our SC model can be interpreted to suggest that sorption occurs when Ca^{2+} at a $>\text{CO}_3\text{Ca}^+$ site is exchanged by EuCO_3^+ or $\text{Eu}(\text{CO}_3)_2^-$, similar to what has been suggested in [30]. For simplicity, we rely solely on the $>\text{Ca}^+$ surface terminations for sorption modeling.

Sorption of Sm to calcite over the range of pH and CO_2 fugacity examined is nearly identical to that of Eu (Figs. 8 and 9). This is consistent with earlier sorption and coprecipitation data [12, 13, 24] as well as speciation data [25]. The unusually high Sm sorption at 24 hours and 0.03% $\text{CO}_2(\text{g})$ results in a higher predicted $>\text{CaCO}_3\text{Sm}(\text{CO}_3)_2^{2-}$ reaction constant when compared to the 0.03% $\text{CO}_2(\text{g})$ Eu and the 1% $\text{CO}_2(\text{g})$ Eu and Sm data (Table 3). The relatively short sorption reaction time (24 hours) should have minimized incorporation of Sm into the calcite solid. However, slight changes in pH or solution conditions may have caused calcite to precipitate and led to greater apparent Sm adsorption. The likelihood that processes other than adsorption affect our sorption results increases with time as radionuclide incorporation into the calcite solid (e.g. [30]) becomes more likely.

Zhong and Mucci [12] measured the sorption of REEs to calcite under seawater conditions, at 0.3% $\text{CO}_2(\text{g})$, and at very high REE concentrations (batch systems where all 12 REEs, each of which was $\sim 6.5 \times 10^{-7}$ mol/L, were introduced simultaneously). Their measured K_d s under these conditions for Sm and Eu were 1800 and 1500 mL/g, respectively. For Sm at pH 8 (the approximate pH of seawater) our measured K_d is 4000 mL/g at 1% $\text{CO}_2(\text{g})$ and > 75000 mL/g at 0.03% $\text{CO}_2(\text{g})$ ¹. While a difference in solution conditions prevent a direct comparison of data, our range of measured values is significantly higher than reported by Zhong and Mucci [12]. The lower values in [12] are likely the result of the very high REE surface loading

¹ At 0.03% $\text{CO}_2(\text{g})$ and pH 8, the aqueous Sm concentration was below our detection limit of 10^{-9} mol/L. Some Sm incorporation into the calcite solid, as a result of calcite precipitation, may have resulted in a Sm K_d significantly higher than Eu. However, slow incorporation into calcite, as described in [30] is not likely due to the short sorption time.

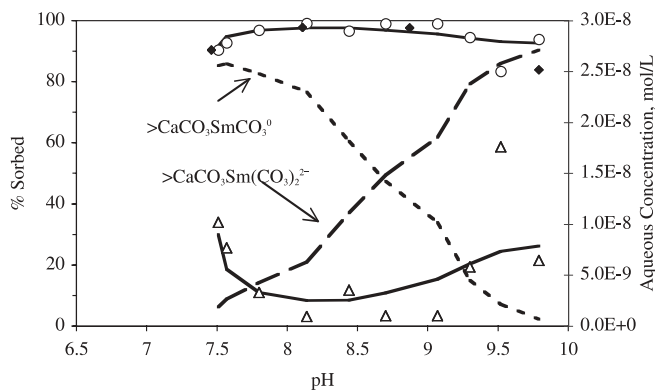


Fig. 8. Sm sorption to calcite at 0.03% $\text{CO}_2(\text{g})$ at 24 hours (O) and 30 days (◆). Lines present total and individual species SC model fits to 24 hour data. Aqueous concentration data (Δ) and overall fit to this data (solid line).

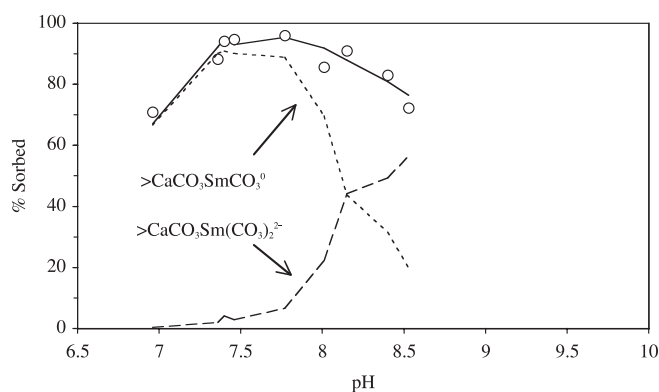


Fig. 9. Sm sorption to calcite at 1% $\text{CO}_2(\text{g})$ at 24 hours (O). Lines present total and individual species SC model fits.

which likely resulted in saturation of calcite surface sites². For Eu at pH 8, our measured K_d is 4000 mL/g at 1% $\text{CO}_2(\text{g})$ and 8000 mL/g at 0.03% $\text{CO}_2(\text{g})$; these values are also significantly higher than those in [12].

3.3 Np sorption to calcite

Np(V) sorption to calcite is much weaker than Sm and Eu and significantly greater pH dependence exists (Fig. 10). Over the pH range examined, the K_d ranges from 0 to 217 mL/g. At the higher and lower pHs, sorption decreases and we attribute this to surface charging and aqueous complexation effects similar to those described for Eu and Sm. Two SC reactions fit the sorption data well but a single SC reaction fit the sorption data nearly equally as well (Table 3). The results presented here suggest that pH and carbonate alkalinity will have a significant effect on Np(V) sorption to calcite.

Keeney-Kennicutt and Morse [8] measured the sorption of Np(V) to a number of minerals in de-ionized water as well as a number of synthetic and natural seawaters (all at pH ~ 8). At very low concentrations (10^{-13} mol/L) in de-ionized water equilibrated with 0.03% $\text{CO}_2(\text{g})$, a K_d of 1815 mL/g was measured compared to 217 mL/g measured here (at pH 8). The difference in sorption affinity is likely

² Note that BET surface areas differed only by a factor of two here and in [12].

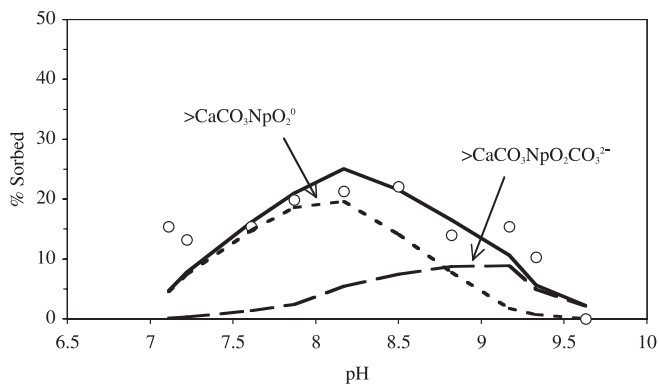


Fig. 10. Np sorption to calcite at 0.03% $\text{CO}_2(\text{g})$ at 24 hours (O). Lines present total and individual species SC model fits.

the result of at least three factors: (a) the surface area of calcite used here is nearly three times lower, (b) a very low Np(V) concentrations was used in Keeney-Kennicutt and Morse [8] and could have resulted in preferential sorption of Np(V) to higher affinity sites, and (c) the solution composition was significantly different. Given the limitations of the comparison, our results are in good agreement with data of Keeney-Kennicutt and Morse [8]. However, our data also show that pH and carbonate alkalinity will greatly affect the affinity of Np(V) for the calcite surface.

3.4 Pu(V) and Pu(IV) sorption

The sorption behavior of Pu(V) at 48 hours is quite similar to Np(V) (Fig. 11). The fitted reaction constant for $>\text{CaCO}_3\text{PuO}_2\text{CO}_3^{2-}$ is also consistent with the parallel Np(V) SC reaction (Table 3). The inclusion of the Pu(V) dicarbonate aqueous species, estimated based on the Np(V) dicarbonate speciation constant, was essential to adequately fit the decreased sorption at high pH. In the case of Pu(V) sorption, only one SC reaction is necessary to adequately fit the sorption data. Also, the measured K_d at pH 8 (~ 20 mL/g) compares favorably with Keeney-Kennicutt and Morse [9] (550 mL/g) when accounting for differences in experimental methods. The methods used by Keeney-Kennicutt and Morse [9] were similar to those described for Np(V) [8] earlier³.

Interestingly, the fraction of Pu(V) sorbed to the calcite surface increases significantly after 7 days. While this may be the result of slow incorporation of Pu(V) into the calcite solid, it may also result from redox changes in Pu as a function of time [26]. At pH 8 and low Pu(V) concentrations, we measured Pu(V) reduction to Pu(IV) at a rate equivalent to $t_{1/2} = 0.2$ years. The slow reduction of Pu(V) to Pu(IV) in solution followed by sorption of Pu(IV) can explain the observed increase in sorption equally well. Increased sorption as a function of time was observed by Keeney-Kennicutt and Morse [9] for Pu(V) sorption to $\delta\text{-MnO}_2$ and goethite (rate of seconds to minutes) and also observed to occur in the presence of calcite at relatively slow rates (days). Since Pu(IV) has a much greater affinity for the calcite surface than Pu(V), the slow reduction of Pu(V) to Pu(IV) in solution [27, 28]

³ The Np(V) comparison yields an order of magnitude difference in K_d which is equivalent to the Pu(V) comparison.

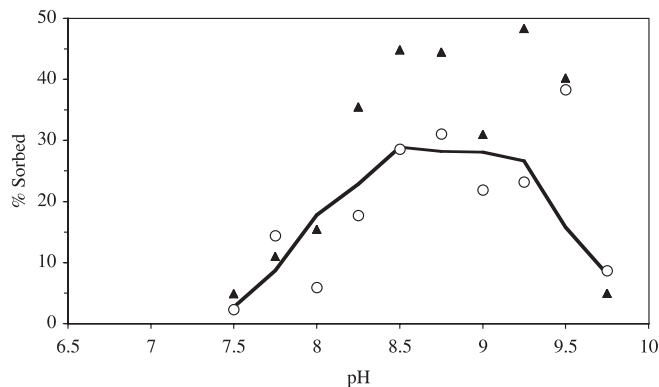


Fig. 11. Pu(V) sorption to calcite at 0.03% $\text{CO}_2(\text{g})$ at 48 hours (O) and 7 days (▲). Line presents SC model fit of $>\text{CaCO}_3\text{PuO}_2\text{CO}_3^{2-}$ species to 48 hour data.

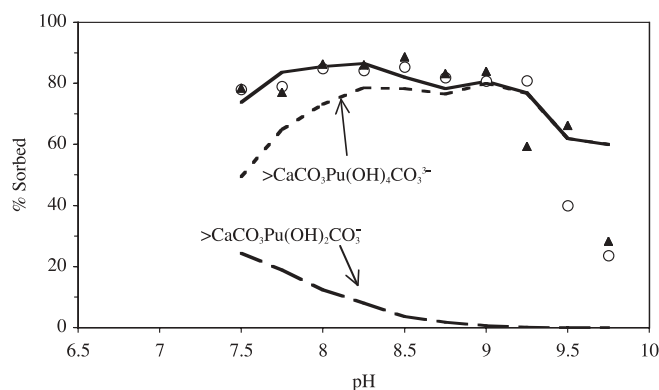


Fig. 12. Pu(IV) sorption to calcite at 0.03% $\text{CO}_2(\text{g})$ at 48 hours (O) and 7 days (▲). Lines present total and individual species SC model fits to 48 hour data.

may result in a slow increase in the overall sorption of Pu to calcite.

The sorption of Pu(IV) to calcite (Fig. 12) is much greater than Pu(V) over the entire pH range examined. However, a decrease in sorption is still observed at low and high pHs. Pu(IV) K_d s range from 60 mL/g at pH 9.75 to 1100 mL/g near pH 8 compared to a range of 5 to 125 mL/g for Pu(V). The agreement between the 48 hour and 7 day sorption data suggest that Pu(IV) is relatively stable both in solution and sorbed to calcite and that incorporation into the calcite solid is not significant over these times. No choice of SC reaction could fit the large decrease in Pu(IV) sorption at high pH. While some decrease in sorption at high pH is predicted with the SC model fit shown in Fig. 12 (reaction constants in Table 3), the decrease does not match the data very well. The limited aqueous Pu(IV) speciation data and the fact that SC modeling cannot fit sorption data at high pH suggests that aqueous species other than those shown in Fig. 5 exist and play a role in the speciation of Pu(IV) at high pH. For example, mono-, di-, or tri-carbonate Pu(IV) species may dominate aqueous speciation at high pH and affect sorption. It may also be that the significant uncertainty in the Pu(IV) hydroxycarbonate and carbonate aqueous speciation constants affects our ability to effectively model the sorption data at high pH.

The data presented here are some of the few data available in the literature regarding REE and actinide sorption to calcite as a function of carbonate alkalinity and pH. Un-

Understanding the effect of solution conditions on sorption is critical to improving our ability to predict the behavior of these elements in the environment. Surface complexation modeling, when coupled with an understanding of aqueous speciation, is an important tool in investigating the factors controlling sorption. Our data suggest that radionuclide sorption to calcite can be an important process controlling the radionuclide transport in the environment and that pH and carbonate alkalinity will affect this process.

Acknowledgment. This work was performed under the auspices of the U.S. Department of Energy by the University of California, Lawrence Livermore National Laboratory under Contract No. W-7405-ENG-48. This research was funded, in part, by the Laboratory Directed Research and Development Program at Lawrence Livermore National Laboratory.

Appendix

Some aqueous species included in Table 1 were based on fits to amorphous PuO_2 solubility data reported in Rai *et al.* [20]. These data were not included in Lemire *et al.* [18] but the aqueous plutonium carbonate species evaluated based on these data are critical to our evaluation of Pu(IV) sorption.

Rai *et al.* [20] examined the solubility of amorphous PuO_2 across a range of pH and carbonate alkalinity conditions. Between pH 8 and 13, the solubility of amorphous PuO_2 remained constant, with an average aqueous Pu(IV) concentration of $10^{-10.4}$ mol/L. This is in good agreement with the predicted solubility based on thermodynamic data in Table 2 ($10^{-10.87}$ mol/L). Upon the addition of carbonate ions in solution, the solubility of amorphous PuO_2 increased dramatically, suggesting the Pu(IV)-carbonate complexation in solution significantly affected PuO_2 solubility. Rai *et al.* [20] fitted Pu(IV) solubility in KHCO_3 (with activity correction based on the Pitzer model) using two aqueous Pu(IV)-carbonate species: $\text{Pu}(\text{OH})_2(\text{CO}_3)_2^{2-}$ and $\text{Pu}(\text{CO}_3)_5^{6-}$. We re-fit this data (with activity correction based on the b-dot model) using the amorphous PuO_2 solubility product reported in Lemire *et al.* [18] (Fig. A1); these reaction constants are listed in Table 1.

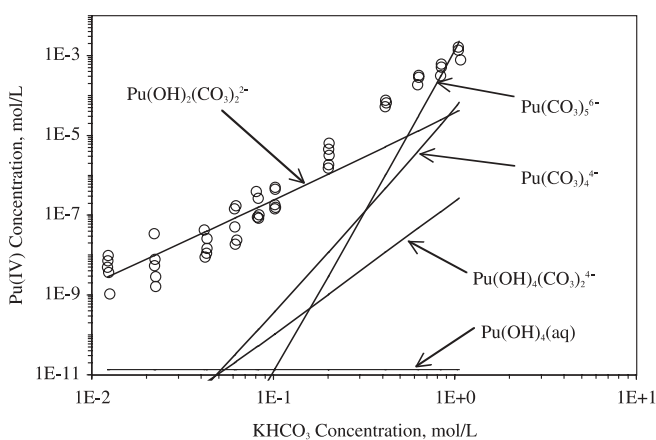


Fig. A1. Fit to amorphous PuO_2 solubility as a function of KHCO_3 concentration. Solubility experiments performed from oversaturation and undersaturation and 5 to 51 day equilibration time. Data from Rai *et al.* [20].

Rai *et al.* [20] also examined amorphous PuO_2 solubility in 0.01 mol/L KOH as a function of K_2CO_3 concentration. These data were not fitted but suggested that a third Pu(IV)-carbonate species may dominate at high pH. We were able to fit this amorphous PuO_2 solubility data using a $\text{Pu}(\text{OH})_4(\text{CO}_3)_2^{4-}$ aqueous species (Figs. A2 and A3). Only the < 1 mol/L K_2CO_3 data were fit since the b-dot activity correction model is unreliable at higher ionic strengths. The 9 day and 49 day equilibrium solubility data resulted in $\text{Pu}(\text{OH})_4(\text{CO}_3)_2^{4-}$ reaction log K constants of 25.7 and 25.4; the average is reported in Table 1. Additional evidence for the existence of this species comes from the data of Yamaguchi *et al.* [22]. Their analysis of amorphous PuO_2 solubility at carbonate/bicarbonate concentrations up to 0.1 molar suggested two dominant Pu(IV)-carbonate species: $\text{Pu}(\text{OH})_2(\text{CO}_3)_2^{2-}$ and $\text{Pu}(\text{OH})_4(\text{CO}_3)_2^{4-}$. We re-fit these data based on the amorphous PuO_2 solubility product reported in Lemire *et al.* [18] which resulted in log K constants of 0.74 and 24.3. These fitted constants are 2.0 and 1.2 log K lower than those based on the data of Rai *et al.* [20]. While the difference is significant, it should not be surprising since the speciation is based relative to the solubility product of amorphous

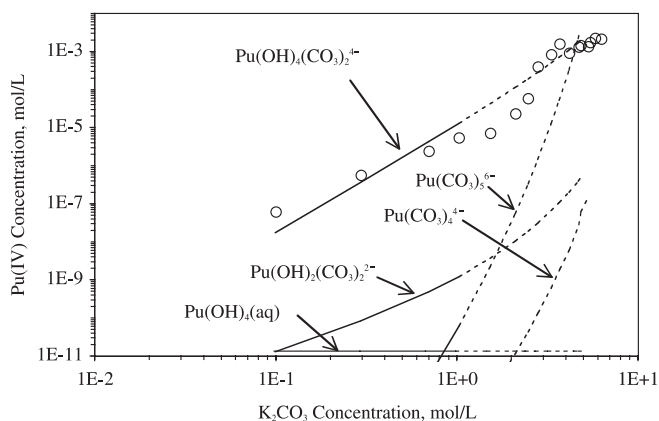


Fig. A2. Fit to amorphous PuO_2 solubility as a function of K_2CO_3 concentration in 0.01 mol/L KOH solution. Solubility experiments performed from oversaturation and 9 day equilibration time. Data from Rai *et al.* [20]. Only < 1 mol/L K_2CO_3 data fitted.

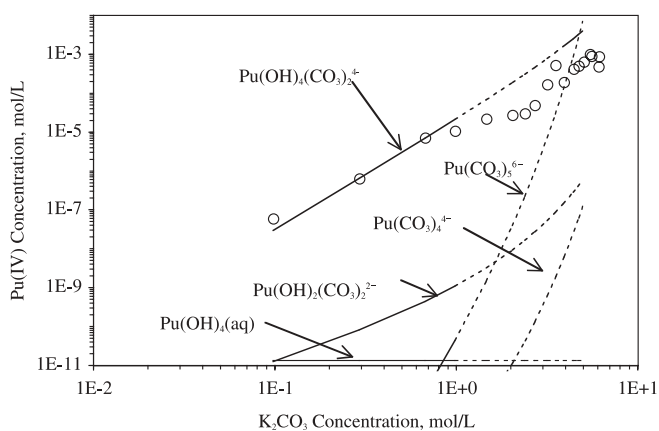


Fig. A3. Fit to amorphous PuO_2 solubility as a function of K_2CO_3 concentration in 0.01 mol/L KOH solution. Solubility experiments performed from oversaturation and 49 day equilibration time. Data from Rai *et al.* [20]. Only < 1 mol/L K_2CO_3 data used in fit.

PuO₂. The variability of amorphous PuO₂ solubility imparts significant uncertainty to the aqueous species reaction constants reported here. Nevertheless, the solubility data of Rai *et al.* [20] and Yamaguchi *et al.* [22] clearly show that carbonate complexation will increase the solubility of amorphous PuO₂ at carbonate concentrations as low as 10⁻³ mol/L. Since the carbonate alkalinity of waters used in the batch sorption experiments reported here is as high as 10⁻¹ mol/L, Pu(IV) hydroxycarbonate or carbonate species will certainly dominate the aqueous speciation for a significant fraction of batch sorption experiments (*i.e.* Fig. 5).

References

- Pokrovsky, O. S., Schott, J.: Surface chemistry and dissolution kinetics of divalent metal carbonates. *Environ. Sci. Technol.* **36**, 426 (2002).
- Slate, J. L.: Buried carbonate paleosols developed in pliocene-pleistocene deposits of the Pasco Basin, South-Central Washington, USA. *Quatern Int.* **34-6**, 191 (1996).
- Robinson, W. L., Conrado, C. L., Hamilton, T. F., Stoker, A. C.: The effect of carbonate soil on the transport and dose estimates from long-lived radionuclides at U.S. Pacific Test Sites. UCRL-JC-130231, Lawrence Livermore National Laboratory, Livermore, CA, USA (1998).
- Carlos, B. A., Chipera, S. J., Bish, D. L.: Distribution and Chemistry of Fracture-Lining Minerals at Yucca Mountain, Nevada. LA-12977-MS, Los Alamos National Laboratory, Los Alamos, USA (1995).
- Zachara, J. M., Cowan, C. E., Resch, C. T.: Sorption of divalent metals on calcite. *Geochim. Cosmochim. Acta* **55**, 1549 (1991).
- Pokrovsky, O. S., Mielczarski, J. A., Barres, O., Schott, J.: Surface speciation models of calcite and dolomite/aqueous solution interfaces and their spectroscopic evaluation. *Langmuir* **16**, 2677 (2000).
- Van Cappellen, P., Charlet, L., Stumm, W., Wersin, P.: A surface complexation model of the carbonate mineral-aqueous solution interface. *Geochim. Cosmochim. Acta* **57**, 3505 (1993).
- Keeney-Kennicutt, W. L., Morse, J. W.: The interaction of Np(V)O₂⁺ with common mineral surfaces in dilute aqueous solutions and seawater. *Marine Chem.* **15**, 133 (1984).
- Keeney-Kennicutt, W. L., Morse, J. W.: The redox chemistry of Pu(V)O₂⁺ interaction with common mineral surfaces in dilute solutions and seawater. *Geochim. Cosmochim. Acta* **49**, 2577 (1985).
- Carroll, S. A., Bruno, J.: Mineral-solution interactions in the U(VI)-CO₂-H₂O system. *Radiochim. Acta* **52**(3), 187 (1991).
- Shanbhag, P. M., Morse, J. W.: Americium interaction with calcite and aragonite surfaces in seawater. *Geochim. Cosmochim. Acta* **46**, 241 (1982).
- Zhong, S. J., Mucci, A.: Partitioning of rare earth elements (REEs) between calcite and seawater solutions at 25-degrees-C and 1 atm, and high dissolved REE concentrations. *Geochim. Cosmochim. Acta* **59**, 443 (1995).
- Curti, E.: Coprecipitation of radionuclides with calcite: Estimation of partition coefficients based on a review of laboratory investigations and geochemical data. *Appl. Geochem.* **14**, 433 (1999).
- Cowan, C. E., Zachara, J. M., Resch, C. T.: Solution ion effects on the surface exchange of selenite on calcite. *Geochim. Cosmochim. Acta* **54**, 2223 (1990).
- Johnson, J. W., Lundeen, S. R.: GEMBOCHS thermodynamic datafiles for use with the EQ3/6 modeling package Lawrence Livermore National Laboratory, Livermore, USA (1997).
- Spahiu, K., Bruno, J.: A selected thermodynamic database for REE to be used in HLNW performance assessment exercises. SKB 95-35, SKB, Stockholm, Sweden (1995).
- Haas, J. R., Shock, E. L., Sassani, D. C.: Rare earth elements in hydrothermal systems – estimates of standard partial molal thermodynamic properties of aqueous complexes of the rare earth elements at high pressures and temperatures. *Geochim. Cosmochim. Acta* **59**, 4329 (1995).
- Lemire, R. J., Fuger, J., Spahiu, K., Nitsche, H., Ullman, W. J., Potter, P., Vitorge, P., Rand, M. H., Wanner, H., Rydberg, J.: *Chemical Thermodynamics of Neptunium and Plutonium*. Elsevier, New York (2001) p. 19.
- Lemire, R. J., Tremaine, P. R.: Uranium and plutonium equilibria in aqueous solutions to 200 °C. *J. Chem. Eng. Data* **25**, 361 (1980).
- Rai, D., Hess, N. J., Felmy, A. R., Moore, D. A., Yui, M., Vitorge, P.: A thermodynamic model for the solubility of PuO₂(am) in the aqueous K⁺-HCO₃⁻-CO₃²⁻-OH⁻-H₂O system. *Radiochim. Acta* **86**, 89 (1999).
- Herbelin, A. L., Westall, J. C., FITEQL: A computer program for determination of chemical equilibrium constants from experimental data. Department of Chemistry, Oregon State University, USA (1994).
- Yamaguchi, T., Sakamoto, Y., Ohnuki, T.: Effect of the complexation of solubility of Pu(IV) in aqueous carbonate system. *Radiochim. Acta* **66/67**, 9 (1994).
- Stipp, S. L. S.: Toward a conceptual model of the calcite surface: Hydration, hydrolysis, and surface potential, *Geochim. Cosmochim. Acta* **63**, 3121 (1999).
- Koepfenkastro, D., Decarlo, E. H.: Sorption of rare-earth elements from seawater onto synthetic mineral particles – an experimental approach. *Chem. Geol.* **95**, 251 (1992).
- Lee, J. H., Byrne, R. H.: Complexation of trivalent rare earth elements (Ce, Eu, Gd, Tb, Yb) by carbonate ions. *Geochim. Cosmochim. Acta* **57**, 295 (1993).
- Kersting, A. B., Zhao, P., Zavarin, M., Sylwester, E. R., Allen, P. A., Williams, R. W.: In: *Colloidal-Facilitated Transport of Low-solubility Radionuclides: A Field, Experimental, and Modeling Investigation*. (Kersting, A. B., Reimus, P. W. E., eds.) Lawrence Livermore National Laboratory, Livermore, California (2003).
- Nitsche, H., Edelstein, N. M.: Solubilities and speciation of selected transuranium ions. A comparison of a non-complexing solution with a groundwater from the Nevada Test Site. *Radiochim. Acta* **39**, 23 (1985).
- Choppin, G. R.: Redox speciation of plutonium in natural waters. *J. Radioanal. Nucl. Chem.* **147**, 109 (1991).
- Mecherri, O. M., Budiman-Sastrowardoyo, P., Rouchard, J., Fedoroff, M.: Study of neodymium sorption on orthose and calcite for radionuclide migration modelling in groundwater. *Radiochim. Acta* **50**, 169 (1990).
- Stumpt, T., Fanghanel, T.: A time-resolved laser fluorescence spectroscopy (TRLFS) study of the interaction of trivalent actinides (Cm(III)) with calcite. *J. Coll. Interface Sci.* **249**, 119 (2002).
- Piriou, B., Fedoroff, M., Jeanjean, J., Bercis, L.: Characterization of the sorption of europium(III) on calcite by site-selective and time-resolved luminescence spectroscopy. *J. Coll. Interface Sci.* **194**, 440 (1997).
- Davis, J., Fuller, C. C., Cook, A. D.: A model for trace metal sorption processes at the calcite surface: Adsorption of Cd²⁺ and subsequent solid solution formation. *Geochim. Cosmochim. Acta* **51**, 1477 (1987).
- Fenter, P., Geissbuhler, P., DiMasi, E., Srajer, G., Sorensen, L. B., Sturchio, N. C.: Surface speciation of calcite observed *in situ* by high-resolution X-ray reflectivity. *Geochim. Cosmochim. Acta* **64**, 1221 (2000).
- Martin-Garin, A., Van Cappellen, P., Charlet, L.: Aqueous cadmium uptake by calcite: a stirred flow-through reactor study. *Geochim. Cosmochim. Acta* **67**, 2763 (2003).
- Kosmulski, M.: Adsorption of trivalent cations on silica. *J. Coll. Interface Sci.* **195**, 395 (1997).